JOURNAL OF APPLIED ELECTROCHEMISTRY 17 (1987) 357–369

A new bath for the electrodeposition of aluminium. II. Kinetics and mechanism of the deposition and dissolution processes

W. A. BADAWY*

Chemistry Department, Faculty of Science, Cairo University, Cairo, Egypt

B. A. SABRAH, N. H. Y. HILAL

Chemistry and Physics Department, Faculty of Education, Cairo University, Fayoum, Egypt

Received 24 March 1986

The electrodeposition of aluminium was carried out successfully in $AlCl_3$–$LiAlH_4$/tetrahydrofuran–toluene solutions. The kinetic parameters controlling the cathodic deposition and anodic dissolution of aluminium were derived. The effect of the total concentration of aluminium and the molar ratio of $AlCl_3$ to $LiAlH_4$ on the current density–potential behaviour of the rotating disc aluminium electrode was also studied. A detailed mechanism for the electrode reactions was suggested.

1. Introduction

The electrodeposition of aluminium from non-aqueous electrolytes is well established [1–4]. One of the best known baths for the electrodeposition of aluminium is the hydride bath, which consists of $AlCl_3$ and $LiAlH_4$ dissolved in tetrahydrofuran (THF) of THF-benzene mixtures [5–9]. Aluminium is deposited from this bath by a continuous process [9]. The deposited films are very pure, fine crystalline, non-porous, silver-white in colour and adherent to the substrate surface [10, 12]. Most of the work carried out in this field has been concerned with the constituents of the electrolytic bath and the practical problems of the electrodeposition of aluminium from THF–hydride baths [1–12]. In a recent paper [13] Graef studied the mechanism of aluminium electrodeposition from solutions of $AlCl_3$ and $LiAlH_4$ in THF. The author claimed that the hydride, present as a catalyst for the electrode reaction, gave rise to instability of the plating bath when present in excess. Also, LiCl and/or LiH were precipitated at the cathode. At the anode, the activation overpotential for the dissolution of aluminium depends on the concentration of the anions AlX_4^- and increases due to the absence of these anions which may lead to the oxidation of the solvent.

In Part I [14] the composition of the hydride bath and its conductivity were examined. It was found that a solution with a total aluminium concentration of 1 mol dm^{-3} and a molar ratio of $LiAlH_4$ to $AlCl_3$ for 1 : 3 in THF–toluene mixture is a good bath for the electrodeposition and electrodissolution of aluminium, not only due to the good conductivity and suitable properties of the bath but also from an economic point of view [14].

In Part II we discuss the kinetics and mechanism of the electrodeposition and electrodissolution of aluminium in the new bath.

2. Experimental details

The potential–current curves were measured under potentiostatic control. The circuit consisted of

0021–891X/87 $03.00 + .12

a potentiostat (FHI G050-17) with an interruption unit to compensate and to measure the ohmic overvoltage accompanying the electrode processes. The interruption of the current was controlled by means of an oscilloscope (Tektronix INC Type 564). The current density–potential curves were traced using an X–Y recorder (JJ PL 50). The measurements of the equilibrium potential were carried out using a high impedance valve voltmeter (Elpo type U 720). The cell used was a double-walled glass cell provided with a light Teflon stopper with suitable openings for the working, counter and reference electrodes and for gas inlets and outlets. To study the transport phenomena a rotating electrode disc of aluminium or aluminized platinum was used as the working electrode. The counter electrodes were made from 99.999% pure aluminium plates. The reference electrode, whether aluminized platinum sheet, $Ag/AgNO_3$ or $Hg/Hg_2(CH_3COO)_2$ was attached to the electrolytic cell through a salt bridge with a Luggin capillary placed almost adjacent to the working electrode.

Materials and solutions were prepared as described previously [14]. All preparations and measurements were carried out under purified nitrogen gas. Copper catalyst and molecular sieves were used to remove the last traces of oxygen or humidity from the inert gas [15]. The composition of the solutions was determined volumetrically, as described elsewhere [10, 16].

3. Results

3.1. *Equilibrium potential measurements*

The equilibrium potential of the aluminium electrode plated *in situ* in $AlCl_3$–$LiAlH_4$/THF–toluene solutions shifts towards more negative values as the total concentration of aluminium in the solution increases at a constant molar ratio of $AlCl_3$ to $LiAlH_4$. On the other hand, at a constant total concentration of aluminium, the equilibrium potential becomes more positive as the molar ratio of $AlCl_3$ to $LiAlH_4$ increases. These results are consistent with those reported recently for the THF bath [13] and those of the THF/benzene solvent [15]. The relation between the equilibrium potential of the aluminium electrode in the $AlCl_3$–$LiAlH_4$ in THF–toluene solutions and the total concentration of aluminium in the bath obeys the familiar Nernst equation [17]. The results of these measurements referred to the normal hydrogen electrode (NHE) are presented in Fig. 1. The Nernstian plot shown in this figure has a slope of -22 mV per decade which corresponds to $n \simeq 3$ for the total number of electrons in the potential-determining electrode process.

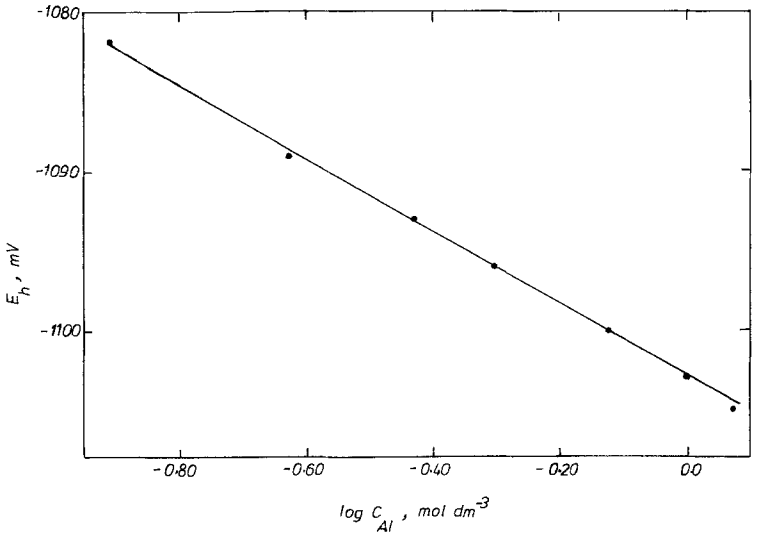

Fig. 1. Variation of the equilibrium potential of the *in situ*-plated aluminium electrode with the total concentration of aluminium (C_{Al}) at a constant molar ratio of $AlCl_3$ to $LiAlH_4$ ($M = 3$) in the $AlCl_3$–$LiAlH_4$/THF–toluene bath at 298 K.

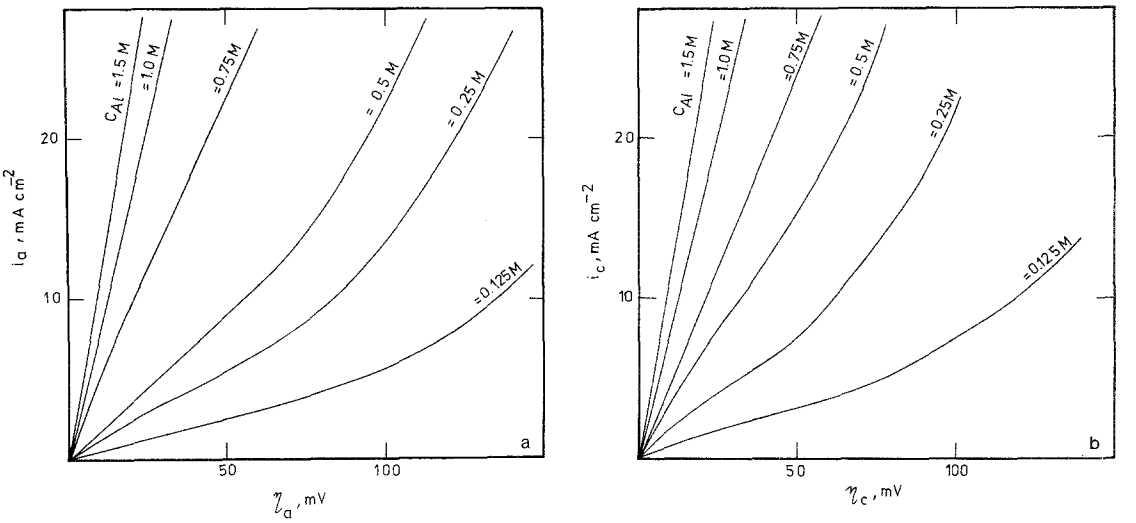

Fig. 2. Current density–potential curves of the rotating disc aluminium electrode in the $AlCl_3$–$LiAlH_4$/THF–toluene bath at $M = 1$ and different values of C_{Al}. Scan rate, 20 mV s^{-1}; rotation speed, 1200 r.p.m.; 298 K. (a) Anodic polarization; (b) cathodic polarization.

The conductivity of the solutions used in this work were as reported in Part I [14]. At a constant molar ratio of $AlCl_3$ to $LiAlH_4$, any increase in the total concentration of aluminium leads to an increase in the conductivity of the solution. The increase of the concentration of $LiAlH_4$ at a constant total concentration of aluminium results in a considerable increase in the conductivity of the solution even when the total concentration of aluminium is low.

3.2. *Polarization measurements*

3.2.1. Effect of total aluminium concentration on current density–potential behaviour. To study the effect of the total aluminium concentration on the current density–potential curves during the cathodic deposition and anodic dissolution of aluminium in the $AlCl_3$–$LiAlH_4$/THF–toluene bath, a series of solutions of constant molar ratio of $AlCl_3$ to $LiAlH_4$ ($M = 1$) and different concentrations (C_{Al}) ranging from 0.125 to 1.5 mol dm^{-3} were prepared. The current density–potential behaviour of the rotating disc aluminium electrode at 298 K, with a rotation speed of 1200 r.p.m. and scan rate of 20 mV s^{-1}, is illustrated in Fig. 2a and 2b for both the anodic and cathodic sides. The general trend in both anodic and cathodic processes is a decrease of overpotential with increase in the total aluminium concentration. At overpotentials higher than ± 60 mV, Tafel regions were obtained.

The solution was well stirred and the speed of rotation of the rotating disc was found to have no effect on the potential–current curves; therefore the electrode processes are not influenced by mass transfer effects [18]. Consequently, the kinetic parameters of the anodic dissolution and cathodic deposition of aluminium were calculated according to the well-known Butler–Volmer equation [17]

$$i = i_0\left[\exp\left(\frac{-\alpha nF\eta}{RT}\right) - \exp\left(\frac{(1-\alpha)nF\eta}{RT}\right)\right] \tag{1}$$

where i is the current density, i_0 the exchange current density, α the transfer coefficient, n the number of electrons transferred in the electrode process, η the overpotential, and F, R and T have their usual meanings. For sufficiently small overpotential, near the equilibrium potential, the linear approxi-

mation of Equation 1 was used for the calculation of the exchange current density:

$$|i| = i_0 \left(\frac{nF}{RT}\right)\eta \tag{2}$$

The ratio η/i in this region is often called the charge transfer resistance, R_{ct}

$$R_{ct} = \left(\frac{RT}{F}\right)\left(\frac{1}{ni_0}\right) \tag{3}$$

The charge transfer resistance serves as a convenient index of kinetic facility [17].

For large values of overpotential where $|\eta| \geqslant 60\,\text{mV}$ the Tafel approximation was used for the calculation of the kinetic parameters, i.e.

$$\eta = a + b \log i \tag{4}$$

where

$$a = \pm\frac{2.303RT}{\alpha nF} \log i_0 = \frac{0.059}{\alpha n} \log i_0 \tag{5}$$

and

$$b = \mp\frac{2.303RT}{\alpha nF} = \frac{0.059}{\alpha n} \tag{6}$$

at 298 K.

The analysis of the current density–potential curves according to Equations 2 and 4 are presented in Figs 3a, 3b, 4a and 4b. It is clear that in all solutions near the equilibrium potential the charge transfer resistance, R_{ct}, diminishes as the total concentration of aluminium increases. Tafel plots were obtained for $C_{Al} \leqslant 0.5\,\text{mol dm}^{-3}$ (Fig. 4a, b).

The different kinetic parameters are summerized in Table 1. The values of i_0 obtained according to Equations 2 or 4 for $C_{Al} \leqslant 0.5\,\text{mol dm}^{-3}$ are comparable.

3.2.2. Effect of molar ratio of $AlCl_3$ to $LiAlH_4$ at constant total aluminium concentration. In this series of experiments the total concentration of aluminium was kept constant at $1\,\text{mol dm}^{-3}$ while the molar ratio (M) $AlCl_3$: $LiAlH_4$ was varied from 5 to 0.333. The current density– potential curves of the anodic and cathodic polarization of the rotating disc aluminium electrode in the different

Table 1. Kinetic parameters for the cathodic deposition and anodic dissolution of aluminium in a $AlCl_3$–$AlClH_4$/THF–toluene bath at constant molar ratio of $AlCl_3$ to $LiAlH_4$ ($M = 1$) and different total concentration of aluminium at 298 K

Total concentration of Al ($mol\,dm^{-3}$)	*Charge transfer resistance* (Ω)		*Exchange current densities* ($mA\,cm^{-2}$)		*Tafel slopes* (mV)	
	$R_{ct(c)}$	$R_{ct(a)}$	$i_{0(c)}$	$i_{0(a)}$	$b_{(c)}$	$b_{(a)}$
1.50	0.9	0.9	21.8	22.2	–	–
1.00	1.3	1.2	15.3	16.5	–	–
0.75	2.2	2.1	9.1	9.8	–	–
0.50	3.0	5.3	6.7	3.7	100	125
0.25	5.7	8.3	3.4	2.2	111	129
0.125	12.5	18.2	1.6	1.0	133	133

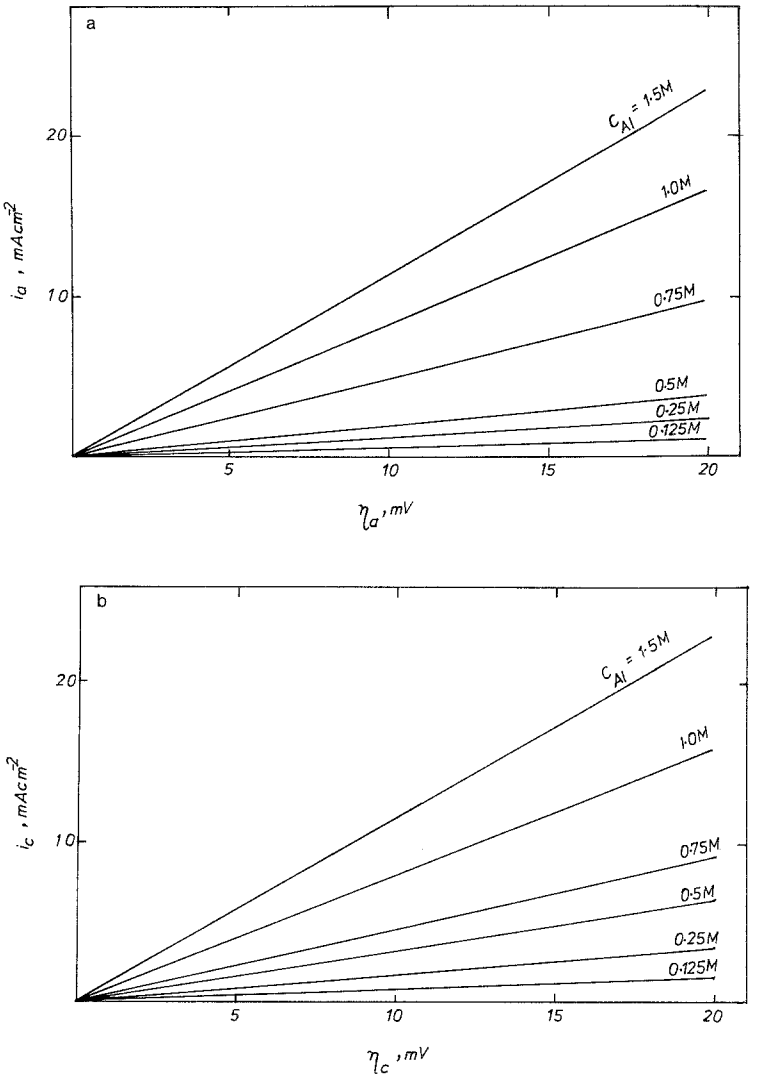

Fig. 3. Linear approximation of the Butler–Volmer equation for the anodic (a) and cathodic (b) polarization of the rotating disc aluminium electrode in the $AlCl_3$–$LiAlH_4$/THF–toluene bath at $M = 1$ and different values of C_{Al}. Scan rate, 20 mV s^{-1}; rotation speed, 1200 r.p.m.; 298 K.

solutions are presented in Fig. 5a and 5b. The analysis of the results according to Equations 2 and 4 are illustrated in Figs. 6a, 6b, 7a and 7b.

It is clear from these results that R_{ct} decreases as the molar ratio decreases, and Tafel plots were obtained for molar ratios of $M \geqslant 3$. The different kinetic parameter of this series are illustrated in Table 2. Again, the exchange current density decreases as the concentration of $LiAlH_4$ in the solution decreases. Also, the exchange current densities obtained according to Equation 2 are more or less the same at those obtained according to Equation 4 for the same solution.

3.3. *Effect of temperature*

The effect of temperature on the current density–potential curves of the cathodic deposition and anodic dissolution of aluminium in the $AlCl_3$–$LiAlH_4$/THF–toluene bath with a constant molar ratio of 3 and a constant total concentration of aluminium of 1 mol dm^{-3} was studied. The results are illustrated in Fig. 8a and 8b. The exchange current density i_0 was found to increase as the temperature increases for both the linear approximation (Fig. 9a, 9b) or the Tafel plots (Fig. 10a,

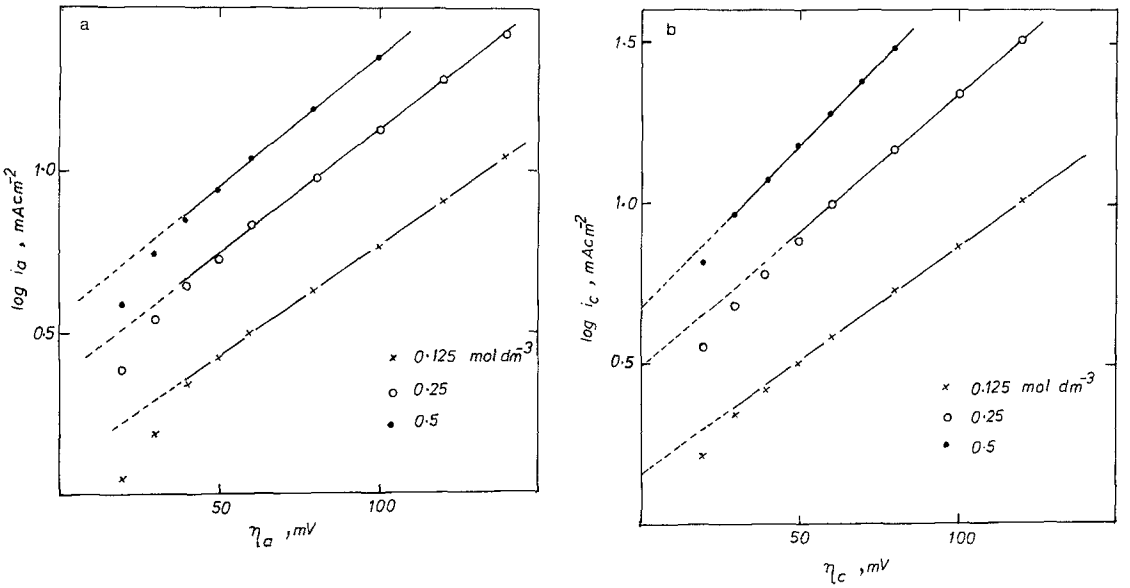

Fig. 4. Tafel plots of the rotating disc aluminium electrode in the $AlCl_3$–$LiAlH_4$/THF–toluene bath at M = 1 and different values of C_{Al}. Scan rate, 20 mV s^{-1}; rotation speed, 1200 r.p.m.; 298 K. (a) Anodic polarization; (b) cathodic polarization.

10b). The charge transfer resistance R_{ct} decreases as the temperature increases (cf. Fig. 9a, 9b). A plot of log $|i_0|$ (either cathodic or anodic) versus $1/T$ gives a straight line that obeys the familiar Arrhenius equation [17],

$$i_0 = A \exp \frac{-E_A}{RT} \tag{7}$$

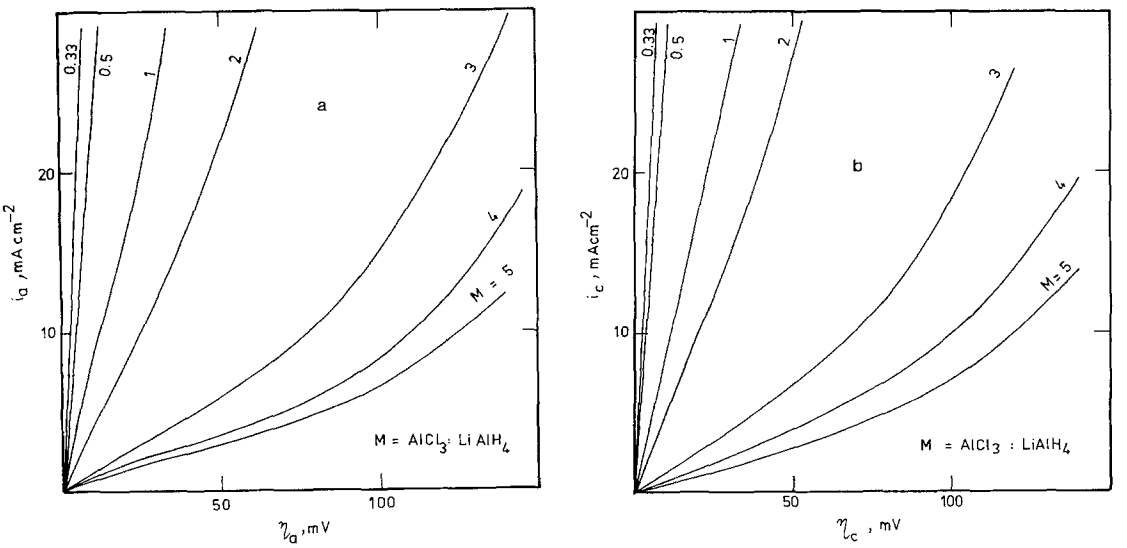

Fig. 5. Current density–potential curves of the rotating disc aluminium electrode in the $AlCl_3$–$LiAlH_4$/THF–toluene bath at constant concentration of aluminium (C_{Al} = 1 mol dm^{-3}) and different molar ratios (M). Scan rate, 20 mV s^{-1}; rotation speed, 1200 r.p.m.; 298 K. (a) Anodic polarization; (b) cathodic polarization.

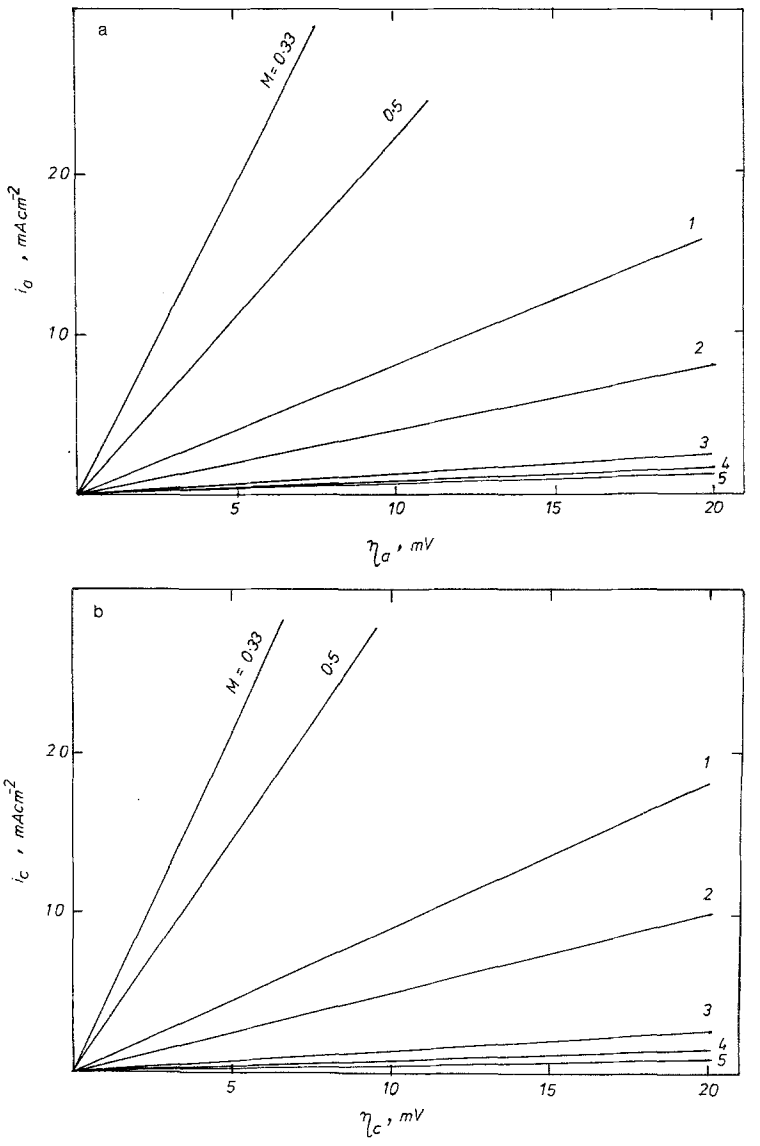

Fig. 6. Linear approximation of the Butler–Volmer equation for the anodic (a) and cathodic (b) polarization of the rotating disc aluminium electrode in the $AlCl_3$–$LiAlH_4$/THF–toluene bath at C_{Al} = 1 mol dm^{-3} and different values of M. Scan rate, 20 mV s^{-1}; rotation speed, 1200 r.p.m.; 298 K.

Table 2. Kinetic parameters for the cathodic deposition and anodic dissolution of aluminium in a $AlCl_3$–$LiAiH_4$/THF–toluene bath at constant total aluminium concentration (C_{Al} = 1 mol dm^{-3}) and different molar ratios of $AlCl_3$ to $LiAlH_4$ (M) at 298 K

Molar ratio (M)	*Charge transfer resistance* (Ω)		*Exchange current densities* (mA cm^{-2})		*Tafel slopes* (mV)	
	$R_{ct(c)}$	$R_{ct(a)}$	$i_{0(c)}$	$i_{0(a)}$	$b_{(c)}$	$b_{(a)}$
5	16.6	14.3	1.2	0.8	133	133
4	12.5	12.5	1.6	0.9	133	121
3	7.7	8.3	2.4	2.6	111	125
2	2.1	2.5	9.8	7.8	–	–
1	1.1	1.25	17.7	15.7	–	–
0.5	0.35	0.45	59.0	43.3	–	–
0.33	0.23	0.25	82.6	76.7	–	–

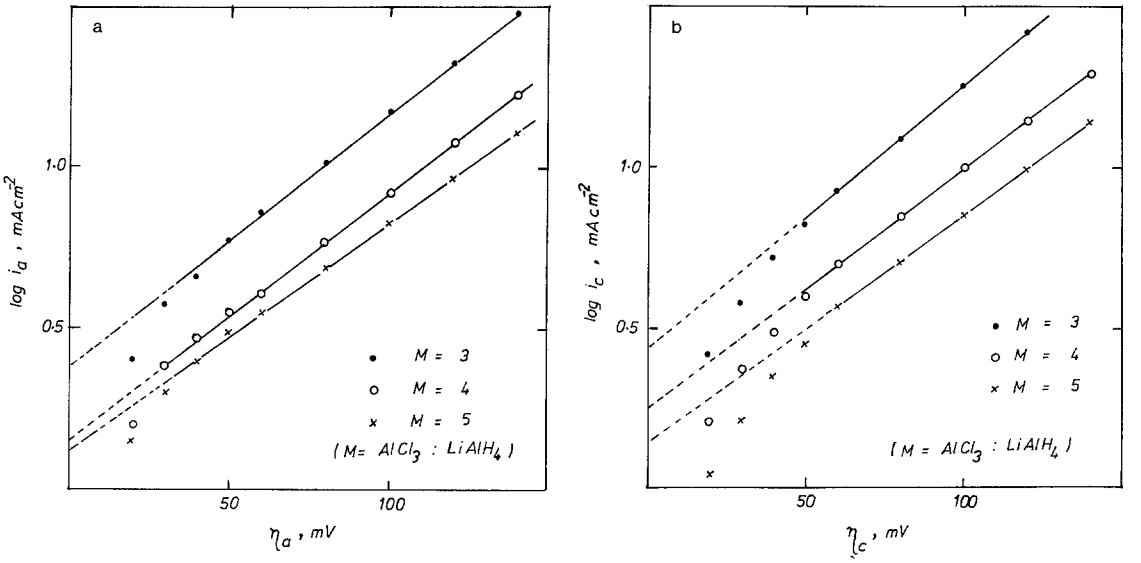

Fig. 7. Tafel plots of the rotating disc aluminium electrode in the $AlCl_3$–$LiAlH_4$/THF–toluene bath at C_{Al} = 1 mol dm^{-3} and different values of M. Scan rate, 20 mV s^{-1}; rotation speed, 1200 r.p.m.; 298 K. (a) Anodic polarization; (b) cathodic polarization.

where E_A is the activation energy and A is the Arrhenius constant or the frequency factor. The activation energy was calculated according to

$$\frac{\mathrm{d} \log i}{\mathrm{d}(1/T)} = \frac{-E_A}{2.303R} \tag{8}$$

The Arrhenius plots for the anodic and cathodic processes are shown in Fig. 11. The values of E_A for the cathodic deposition and anodic dissolution of aluminium in the bath together with the other

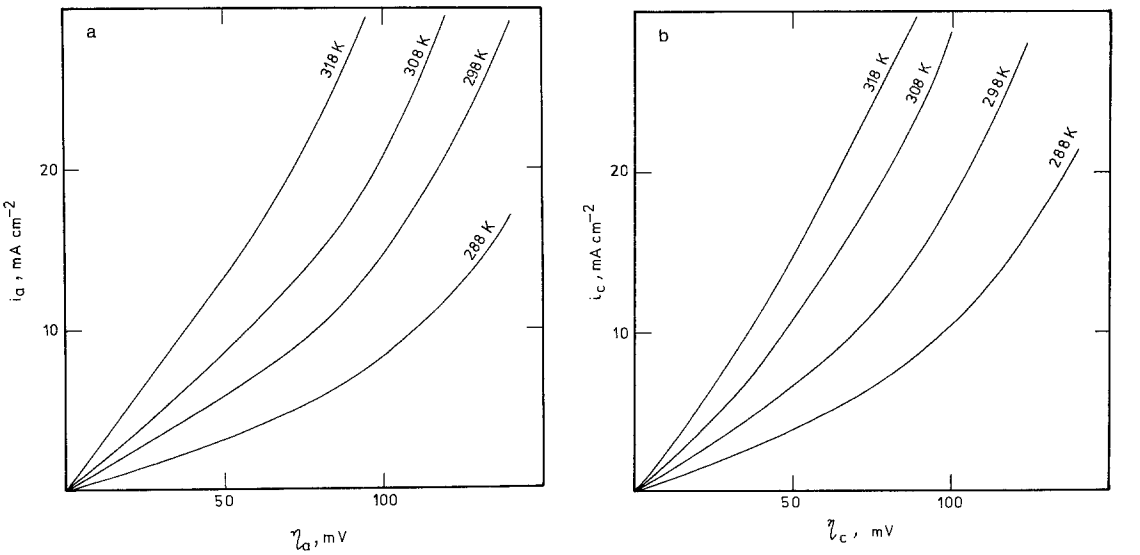

Fig. 8. Effect of temperature on the current density-potential behaviour of the rotating disc aluminium electrode in the $AlCl_3$–$LiAlH_4$/THF–toluene bath at C_{Al} = 1 mol dm^{-3} and M = 3. Scan rate, 20 mV s^{-1}; rotation speed 1200 r.p.m. (a) Anodic polarization; (b) cathodic polarization.

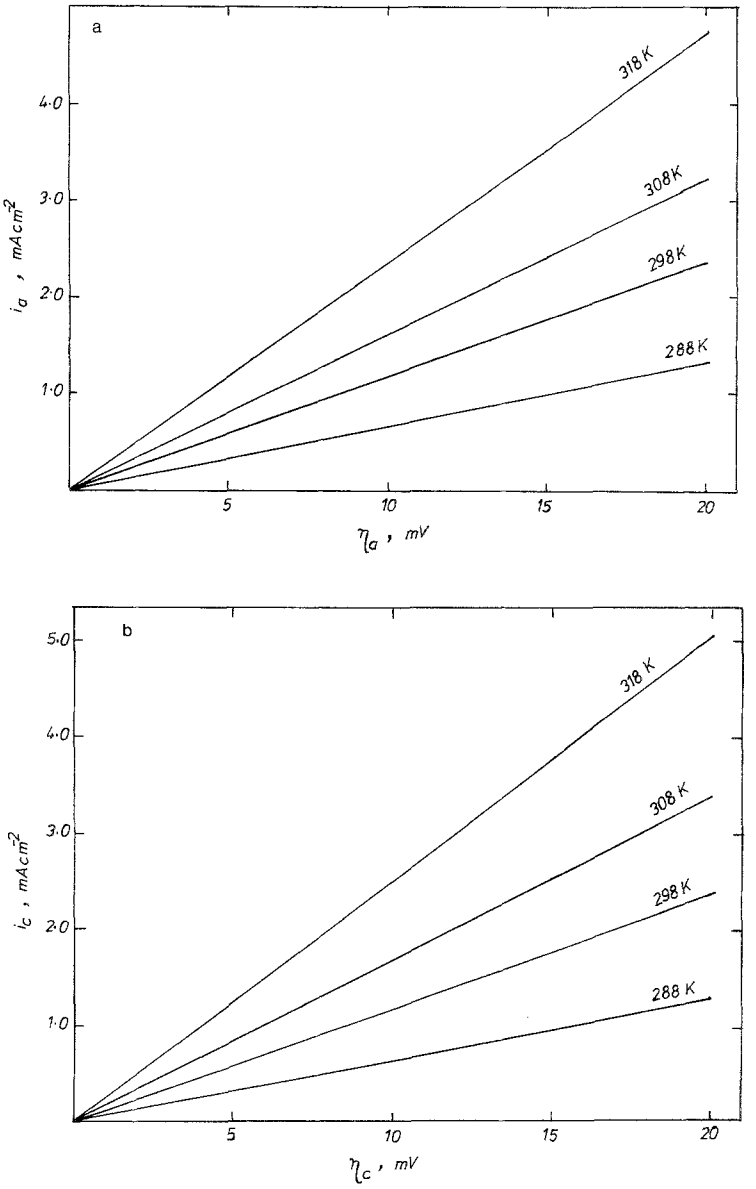

Fig. 9. Linear approximation of the Butler–Volmer equation for the anodic (a) and cathodic (b) polarization of the rotating disc aluminium electrode in the $AlCl_3$–$LiAlH_4$/THF–toluene bath at $C_{Al} = 1\,mol\,dm^{-3}$, $M = 3$ and different temperatures. Scan rate, $20\,mV\,s^{-1}$; rotation speed, 1200 r.p.m.

kinetic parameters are illustrated in Table 3. The values of i_0 obtained according to Equation 2 are more or less the same as those obtained according to Equation 4 for the same temperature.

4. Discussion

Conductivity and equilibrium potential measurements together with the analysis of the electrode compartments during polarization indicate that aluminium is present in anionic forms which participate in the equilibrium process at the aluminium electrode. The results of polarization measurements show that the electrode reactions are affected by the composition of the solution. The composition of the bath and hence the anions and cations therein depend essentially on the molar ratio of $AlCl_3$ to $LiAlH_4$ [7, 11–15, 19].

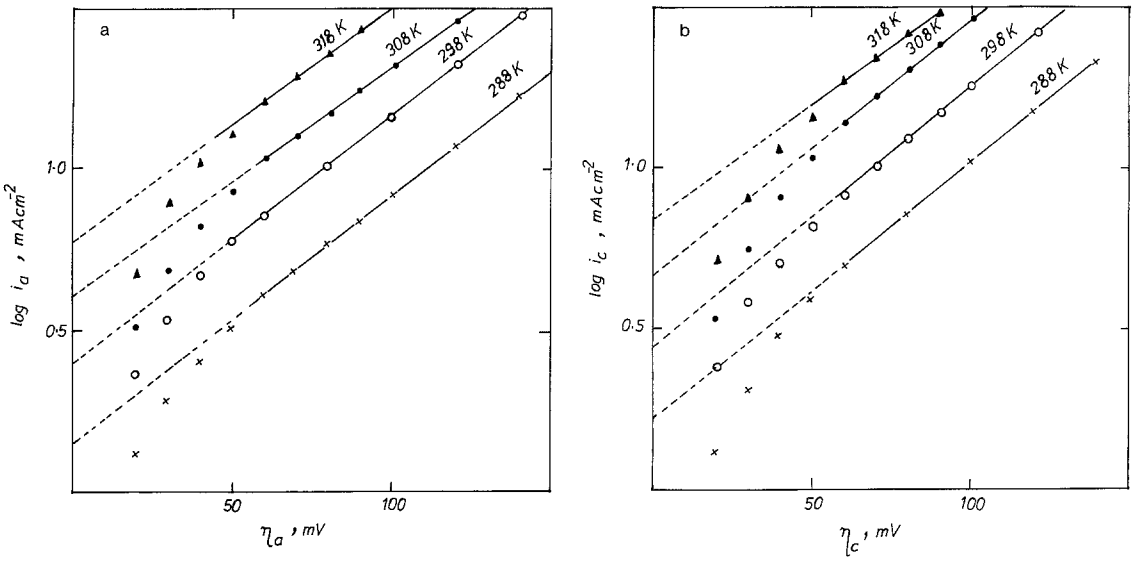

Fig. 10. Tafel plots for the anodic (a) and cathodic (b) polarization of the rotating disc aluminium electrode at different temperatures, when $C_{Al} = 1\,mol\,dm^{-3}$ and $M = 3$. Scan rate, $20\,mV\,s^{-1}$; rotation speed, 1200 r.p.m.

Table 3. Kinetic parameters for the cathodic deposition and anodic dissolution of aluminium in a $AlCl_3$–$LiAlH_4$/THF–toluene bath at a constant molar ratio (M = 3) and constant total aluminium concentration, $C_{Al} = 1\,mol\,dm^{-3}$, at different temperatures

Temperature (K)	*Charge transfer resistance* (Ω)		*Exchange current densities* ($mA\,cm^{-2}$)		*Tafel slopes* (*mV*)		*Activation energy* ($kJ\,mol^{-1}$)	
	$R_{ct(c)}$	$R_{ct(a)}$	$i_{0(c)}$	$i_{0(a)}$	$b_{(c)}$	$b_{(a)}$	$E_{A(c)}$	$E_{A(a)}$
288	15.4	15.4	1.6	1.5	133	133		
298	8.3	8.7	2.75	2.45	125	125	38.2	36.3
308	5.4	6.2	4.60	4.00	125	133		
318	3.9	4.3	7.25	6.00	133	133		

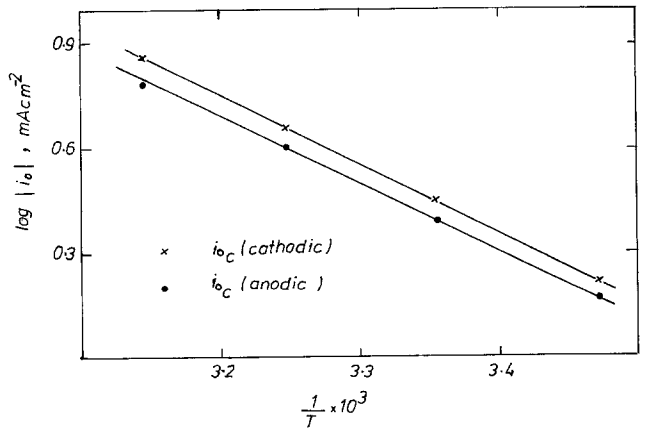

Fig. 11. Log $|i_0|$ vs $1/T$ plots for the cathodic deposition and anodic dissolution of aluminium in the $AlCl_3$–$LiAlH_4$/THF–toluene bath, when $C_{Al} = 1\,mol\,dm^{-3}$ and $M = 3$.

Thus for $M = 3$:

$$LiAlH_4 + 3AlCl_3 \longrightarrow 3AlHCl_2 + Li^+ + AlHCl_3^- \quad (9)$$

for $M = 1$:

$$LiAlH_4 + AlCl_3 \longrightarrow AlH_2Cl + Li^+ + AlH_2Cl_2^- \quad (10)$$

and for $M = 0.33$:

$$3LiAlH_4 + AlCl_3 \longrightarrow AlH_3 + 3Li^+ + 3AlH_3Cl^- \quad (11)$$

Reactions 9–11 show that the aluminium is present in anionic or neutral forms. Even the neutral molecules undergo disproportionation and react with the electrolysis products such as H^- or Cl^- leading to formation of cationic and anionic species (reactions 12–19) which are responsible for the increased conductivity of the solution as discussed in Part I [14]. These species also participate in the electrode reactions:

$$AlHCl_2 + H^- \longrightarrow AlH_2Cl_2^- \quad (12)$$

$$AlHCl_2 + Cl^- \longrightarrow AlHCl_3^- \quad (13)$$

$$AlH_2Cl + H^- \longrightarrow AlH_3Cl^- \quad (14)$$

$$AlH_2Cl + Cl^- \longrightarrow AlH_2Cl_2^- \quad (15)$$

$$AlH_3 + Cl^- \longrightarrow AlH_3Cl^- \quad (16)$$

$$AlH_3 + H^- \longrightarrow AlH_4^- \quad (17)$$

$$2AlHCl_2 \longrightarrow AlH_2Cl_2^- + AlCl_2^+ \quad (18)$$

$$2AlH_2Cl \longrightarrow AlH_2Cl_2^- + AlH_2^+ \quad (19)$$

The participation of the aluminium-containing ions in the electrode reactions is not restricted to the transport of the charge only. The dependence of the overpotential accompanying the electrode processes on the composition of the solution may be attributed to the presence of the different anionic species in the different solutions. Thus, in solutions with molar excess of $LiAlH_4$, the smaller and less stable anion AlH_3Cl^- is present as the main anion, whereas in solutions with molar excess of $AlCl_3$, the bulky $AlHCl_3^-$ is the predominant anion. The transfer of an electron to the bulky $AlHCl_3^-$ anion is accompanied by high overvoltage due to its relative stability and steric hindrance. The transfer of the electron to the smaller anion AlH_3Cl^- is easier and occurs with very little overvoltage. This explains why the overvoltage increases as the molar ratio of $AlCl_3$ increases (cf. Fig. 5a, 5b). It indicates also that $LiAlH_4$ is present not only as a catalyst for the electrode processes [13] but also as an essential participant in the formation of the ions responsible for the good conductivity of the bath and is important for the electrodeposition of aluminium as well. As the molar ratio of $LiAlH_4$ increases the concentration of the mobile ions increases and hence higher conductivity [14] and low overpotential for the cathodic deposition and also for the anodic dissolution of aluminium is achieved.

Since the current density–potential curves are not affected by the speed of rotation of the rotating disc electrode, the presence of concentration overpotential is excluded [18]. Thus, the observed overpotential is either due to charge transfer resistance or activation polarization.

In solutions with molar excess of $LiAlH_4$, activation overpotential has not been observed. It follows that in these solutions neither transport processes nor activation overpotential play an important role in the determination of the reaction rate. In general, the overall mechanism of the electrode process involves consecutive electron transfer steps. The transfer of the first electron to the reacting species is considered to be the rate determining step (r.d.s.). The relation between the overall

charge transfer coefficients $\alpha_{(c)}$ (for the cathodic reaction), $\alpha_{(a)}$ (for the anodic reaction) and the symmetry factor, β, may be given by

$$\alpha_{(c)} = \frac{\gamma_p}{\nu} + \beta r \tag{20}$$

$$\alpha_{(a)} = \frac{\gamma_f}{\nu} + (1 - \beta)r \tag{21}$$

where γ_p = the number of electrons transferred in the steps preceding the r.d.s., γ_f = the number of electrons transferred in the steps following the r.d.s., and r is the number of electrons transferred in the r.d.s. itself. The stoichiometric number of the r.d.s. is given by ν [20, 21]. The total number of transferred electrons, n, is then given by

$$n = \gamma_p + \nu r + \gamma_f \tag{22}$$

The results presented in Figs 2a, 2b, 5a, 5b, 8a and 8b show that the anodic and cathodic current density–potential curves are more or less symmetrical. The anodic and cathodic exchange current densities, $i_{0(a)}$ and $i_{0(c)}$, as well as the anodic and cathodic Tafel slopes, $b_{(a)}$ and $b_{(c)}$, together with the values of the activation energy for the cathodic deposition and anodic dissolution of aluminium (cf. Tables 1–3), point to a one-electron transfer being the r.d.s. in the electrode process [21–23]. The experimental and theoretical values of the transfer coefficients, $\alpha_{(a)}$ and $\alpha_{(c)}$, calculated according to Equations 18 and 19 ($\alpha_{(a)} = \alpha_{(c)} = 0.5$), indicate that the transfer of the first electron is the r.d.s. This is in good agreement with the derivations of Lovrečček [24] and Wright [25] for the calculation of the Tafel slope, b, in multi-electron processes.

The mechanism of the cathodic deposition of aluminium from the $AlCl_3$–$LiAlH_4$/THF–toluene bath may be written as:

(i) The rate determining step (r.d.s.) (slow):

$$\left.\begin{array}{lll} M = 3; & AlHCl_3^- + e \longrightarrow & AlHCl + 2Cl^- \\ M = 1; & AlH_2Cl_2^- + e \longrightarrow & AlH_2 + 2Cl^- \\ M = 0.33; & AlH_3Cl^- + e \longrightarrow & AlH_2 + Cl^- + H^- \end{array}\right\} \tag{23}$$

(ii) Consecutive reactions (fast):

(a)
$$\left.\begin{array}{l} AlH_2 + e \longrightarrow Al^+ + 2H^- \\ AlHCl + e \longrightarrow Al^+ + H^- + Cl^- \end{array}\right\} \tag{24}$$

(b)
$$Al^+ + e \longrightarrow Al$$

The overall electrode reaction may be written as

$$AlX_4^- + 3e \longrightarrow Al + 4X^- \tag{25}$$

where X is either H or Cl. The resulting H^- and Cl^- react directly with the neutral species (cf. Equations 12–17) to give the aluminium-containing anions and the reaction continues. Since the electrode reactions are symmetrical the anodic reaction will be the mirror image of the cathodic reaction and the transfer of the first electron will be the rate determining dissolution step. Thus

(i) The r.d.s. (slow):

$$Al \longrightarrow Al^+ + e \tag{26}$$

(ii) Consecutive reactions (fast):

(a)
$$Al^+ + 2X^- \longrightarrow AlX_2 + e \tag{27}$$

(b)
$$AlX_2 + 2X^- \longrightarrow AlX_4^- + e \tag{28}$$

The overall dissolution reaction is

$$Al + 4X^- \longrightarrow AlX_4^- + 3e \tag{29}$$

Therefore, the anodic dissolution and cathodic deposition of aluminium from the $AlCl_3$–$LiAlH_4$/THF–toluene bath may be represented simply as

$$AlX_4^- + 3e \underset{\text{anodic dissolution}}{\overset{\text{cathodic deposition}}{\rightleftharpoons}} Al + 4X^- \tag{30}$$

References

[1] B. S. Del Duca, *J. Electrochem. Soc.* **118** (1971) 405.
[2] R. K. Willardson and H. L. Georing (eds), 'Compound semiconductors', Vol. 1, Reinhold, New York (1962).
[3] D . E. Couch and A. Brenner, *J. Electrochem. Soc.* **99** (1952) 234.
[4] J. H. Connor and A. Brenner, *ibid.* **103** (1956) 657.
[5] N. Ishibashi, Y. Hanamura, M. Yoshio and T. Seiyama, *Denki Kagaku* **37** (1969) 73.
[6] N. Ishibashi and M. Yoshio, *Electrochim. Acta* **17** (1972) 1343.
[7] M. Kocke and S. Sekimoto, *Kinzoku* **42** (1972) 77.
[8] Y. Matsuda, Y. Öuchi and H. Tamura, *J. Appl. Electrochem.* **4** (1974) 53.
[9] J. G. Beach, L. D. McGraw and C. L. Faust, *Plating* **55** (1968) 936.
[10] F. A. Clay, W. B. Harding and C. T. Stimetz, *ibid.* **56** (1969) 1027.
[11] E. C. Ashby and J. Prather, *J. Amer. Chem. Soc.* **88** (1966) 729.
[12] M. Yoshio, H. Miura, N. Ishibashi and E. Takeshima, *J. Inorg. Nucl. Chem.* **38** (1976) 2314.
[13] M. W. M. Graef, *J. Electrochem. Soc.* **132** (1985) 1038.
[14] W. A. Badawy, B. A. Sabrah and N. H. Y. Hilal, *J. Appl. Electrochem.* **16** (1986) 707.
[15] Diss. W. A. Badawy, TH 'Carl Schorlemmer' Ieuna Merseburg – GDR (1980).
[16] W. Fresenius and G. Jander, 'Handbuch der Analytischen Chemie' Vol. 3, Springer-Verlag, Berlin (1972) part III/aα_2, p. 220 and part VII /aβ_2, p. 96.
[17] A. J. Bard and L. R. Faulkner, 'Electrochemical Methods – Fundamentals and Applications', John Wiley and Sons, New York (1980), chap. 3.
[18] L. I. Antropov, 'Theoretical Electrochemistry', Mir Publishers, Moscow (1972), chap. 14.
[19] M. Yoshio, N. Ishibashi, H. Waki and T. Seiyama, *J. Inorg. Nucl. Chem.* **34** (1972) 2439.
[20] J. O'M. Bockris and A. Reddy, 'Modern Electrochemistry', Plenum Press, New York (1972) p. 1006.
[21] K. J. Vetter, 'Electrochemical Kinetics – Theoretical and Experimental Aspects', Academic Press, New York, London (1967), chap. 3.
[22] T. Erdey-Grüz, 'Kinetics of Electrode Processes', Akdemiai kiadó, Budapest (1975) pp. 68.
[23] J. O'M. Bockris and G. A. Razumney, 'Fundamental Aspects of Electrocrystallization', Plenum Press, New Yrok (1967) p. 36.
[24] B. Lovreček, *J. Phys. Chem.* **63** (1959) 1975.
[25] G. A. Wright, *J. Electrochem. Soc.* **114** (1967) 1263.